A survey of gradual solar energetic particle events

L. Barnard[1] and M. Lockwood[1]

Received 21 September 2010; revised 8 February 2011; accepted 16 February 2011; published 11 May 2011.

[1] We develop a database of 110 gradual solar energetic particle (SEP) events, over the period 1967–2006, providing estimates of event onset, duration, fluence, and peak flux for protons of energy E > 60 MeV. The database is established mainly from the energetic proton flux data distributed in the OMNI 2 data set; however, we also utilize the McMurdo neutron monitor and the energetic proton flux from GOES missions. To aid the development of the gradual SEP database, we establish a method with which the homogeneity of the energetic proton flux record is improved. A comparison between other SEP databases and the database developed here is presented which discusses the different algorithms used to define an event. Furthermore, we investigate the variation of gradual SEP occurrence and fluence with solar cycle phase, sunspot number (SSN), and interplanetary magnetic field intensity (B_{mag}) over solar cycles 20–23. We find that the occurrence and fluence of SEP events vary with the solar cycle phase. Correspondingly, we find a positive correlation between SEP occurrence and solar activity as determined by SSN and B_{mag}, while the mean fluence in individual events decreases with the same measures of solar activity. Therefore, although the number of events decreases when solar activity is low, the events that do occur at such times have higher fluence. Thus, large events such as the "Carrington flare" may be more likely at lower levels of solar activity. These results are discussed in the context of other similar investigations.

Citation: Barnard, L., and M. Lockwood (2011), A survey of gradual solar energetic particle events, *J. Geophys. Res.*, *116*, A05103, doi:10.1029/2010JA016133.

1. Introduction

[2] Solar energetic particle (SEP) events are a particular hazard in the near-Earth space environment. A typical event consists of an enhancement to the flux of energetic particles in the *keV* to *GeV* energy range, which can be orders of magnitude in amplitude and persists over a time scale of hours to days. The particle population of an event at Earth is dependent on the location of the particle acceleration within the heliosphere, which occurs in both the solar corona and interplanetary space. Consequently the majority of SEPs are protons, although there are an appreciable fraction of heavier nuclei too [*Reames*, 1998]. The particle acceleration broadly falls into two categories; particles accelerated at the site of a solar flare in the solar corona, or particles accelerated on a shock wave propagating through the solar corona or interplanetary space: generally speaking, these give two classes of SEP events; impulsive SEP events and gradual SEP events, respectively.

[3] In impulsive events particles are accelerated stochastically via resonant wave interactions in a localized region at the footprint of a solar flare [*Reames*, 1999] and in reconnecting current sheets above flaring loops [*Zharkova and Gordovskyy*, 2004]. Energized particles may then stream out to 1 *AU* on open field lines connected to this region, typically spanning 20° of solar longitude [*Reames*, 2002]. On the other hand, gradual events are driven by acceleration at shocks ahead of both coronal mass ejections (CMEs) and corotating interaction regions (CIRs): these may extend over 100° of solar longitude and can propagate out past 1 *AU*. In this instance energetic particles may be observed either remotely, by being magnetically connected to the shock front, or directly by passing through the propagating shock wave.

[4] An SEP event may consist of both impulsive and gradual components, but it is found that of the two classes gradual events have a longer time scale (days) and larger peak fluxes [*Kallenrode*, 2003]. Therefore gradual SEP events generally produce a higher fluence (the time integral of flux) than impulsive events. Large fluences of energetic charged particles are an important consideration in the design of any space-bound technology [*Gubby and Evans*, 2002] and are a severe radiation hazard to astronauts [*Townsend et al.*, 1991]. This is particularly the case for any missions which necessitate leaving the radiation protection of the Earth's magnetosphere. This shield is, however, only partial and so despite the protection of the Earth's magnetosphere, SEPs can penetrate the Earth's atmosphere, and can contribute significantly to the radiation dose received by passengers aboard high-altitude aircraft [*Dyer et al.*, 2003; *Mertens et al.*, 2010] as well as for astronauts in low Earth orbit. This has motivated the inclusion of SEP events into atmospheric radiation models [*Dyer et al.*, 2009].

[1]Department of Meteorology, University of Reading, Reading, UK.

0148-0227/11/2010JA016133

Table 1. Spacecraft Contributing to the (>60 MeV) Proton Flux Record in OMNI 2

Mission	Start	End
IMP 4	30 May 1967	3 May 1969
IMP 5	21 Jun 1969	24 Dec 1972
IMP 7	2 Oct 1972	31 Oct 1978
IMP 8	26 Oct 1973	1 Jan 2006
GOES 11	1 Jan 2006	1 Jan 2007

[5] SEP events also have geophysical interactions. The generation of odd nitrogen (NO_y) by SEPs, in the mesosphere and stratosphere [*Mlynczak et al.*, 2003], leads to the dissociation of ozone in the stratosphere, as discussed by *Jackman et al.* [2009]. This perturbation to stratospheric ozone is strongest near the poles (where geomagnetic shielding of SEPs is weakest) and can last for months. It is not yet understood if energetic charged particle precipitation has any further ramifications on Earth's weather and climate, however some research suggests it may have an appreciable effect in the polar troposphere [*Seppälä et al.*, 2009].

[6] SEP events are observed in a variety of ways. Direct observation is achieved both in space and in the atmosphere. Energetic particle detectors aboard space craft have been recording the near-Earth energetic particle flux for different energy and mass ranges since the mid 1960's. Alongside this, high-altitude balloon flights carrying Geiger tubes have also recorded SEP activity in the atmosphere since 1957 [*Bazilevskaya et al.*, 2010]. Furthermore, since the work of *Forbush* [1946] we know that sufficiently large enough SEP events cause nuclear reactions in the upper atmosphere, giving enhancements to the flux of neutrons measured by ground-based neutron monitors (these are called ground level enhancements, GLEs). The NO_y generated in the middle atmosphere by SEP events also precipitates down into polar ice. Hence, polar ice cores yield a list of historic SEP events [*Shea et al.*, 1998; *Shea and Smart*, 2004], although these events must be particularly large to detectably perturb the background nitrate level in the ice sheets.

[7] This paper aims to utilize the direct observations of SEP events in space, by a variety of missions, to establish a reliable and homogenous database of gradual SEP events to aid further investigation of the phenomenon and its effects. Section 2 describes the data sources used and the analysis of the energetic proton flux, while section 2.2 describes the specific algorithm developed to extract gradual SEP events from the energetic particle flux. A comparison of the database of gradual SEPs developed here with other databases of SEP events (defined using different criteria) formed from direct observations is also presented. Section 3 analyzes the variation in occurrence and fluence of SEP events over solar cycles 20 to 23 and, in particular, the variation with respect to the solar cycle phase, sunspot number and near-Earth interplanetary magnetic field (IMF) magnitude (B_{mag}). A discussion of our results, and how they compare with similar research, is included in section 4.

2. Data and Analysis

2.1. Intercalibration of Different Data Sources

[8] The OMNI 2 data set, provided by the Space Physics Data Facility (SPDF) of NASA's Goddard Space Flight Center, is a valuable resource for the investigation of solar energetic particles. Included in the data set are energetic proton flux measurements at hourly resolution which extend from 1967 up to the present day. Over this period, multiple spacecraft have been used to compile the composite energetic proton flux data set. Table 1 summarizes the spacecraft used and the periods over which they contributed to the OMNI 2 data set. The data set and supporting documentation can be found on the OMNIWeb Web site (http://omniweb.gsfc.nasa.gov/ow.html). Note that the OMNI 2 data set used here was downloaded on 1 December 2010 and contains recent improvements, including the removal of some spurious spikes.

[9] The energetic proton flux is given in six integral energy bands, which are for energies (E) exceeding thresholds of 1, 2, 4, 10, 30 and 60 MeV. The hourly mean proton flux for $E > 60$ MeV, provided by the OMNI 2 data composite, is displayed in Figure 1. It is apparent from Figure 1 that the character of the data occasionally changes abruptly. These jumps are frequently coincident with changes in the instrumentation used.

[10] For a statistical investigation of gradual SEP events, and to automate event detection, it is important that the data set be as homogenous as possible. Although the OMNI 2 record is already very useful for the investigation of gradual SEP events, changes in character of the data mean it may potentially be improved upon for long-term studies. In addition, due to tracking limitations and other factors, there are frequent gaps in the data series, particularly between 1983 and 1995 [*Finch and Lockwood*, 2007]. Most of these data gaps, but not all, are shorter than the typical gradual SEP duration of a few days.

[11] Data contributed to the proton flux record from the IMP craft are measured in a geocentric orbit of approximately 30 Earth radii. The majority of this orbit is outside the magnetosphere in the solar wind, however approximately 35% of the 12.5 day orbit was spent crossing the magnetotail. Due to the energies (>60 MeV) of the particles being studied and the large orbital radius of the satellite, we consider these measurements as taken outside effective magnetospheric shielding. However, the data provided by GOES 11 are measured in geostationary orbit which is, except for very rare dayside observations during events of exceptionally high solar wind dynamic pressure, inside the magnetosphere. Due to the fragmented coverage provided by IMP 8 after late 2001, data from GOES 11 becomes increasingly common in the data set until by the beginning of 2006 this satellite is the sole data contributor. The different locations of IMP 8 and GOES 11 craft mean that the data sequences have fundamental differences as well as similarities. Because of this, analysis of the flux record is here split in two sections. Initially the data contributed by IMP craft up to 2001 is processed, and subsequently the period containing both IMP 8 and GOES 11 data after 2001 is handled.

[12] It is assumed that long-term variation in the background proton flux in the IMP data (seen between SEP events) is due to solar wind modulation of the local galactic cosmic ray spectrum (GCR). Neutron monitors (NMs) on Earth's surface indirectly measure the solar wind modulation of the local GCR spectrum by detecting neutrons generated when cosmic rays hit the atmosphere. We here

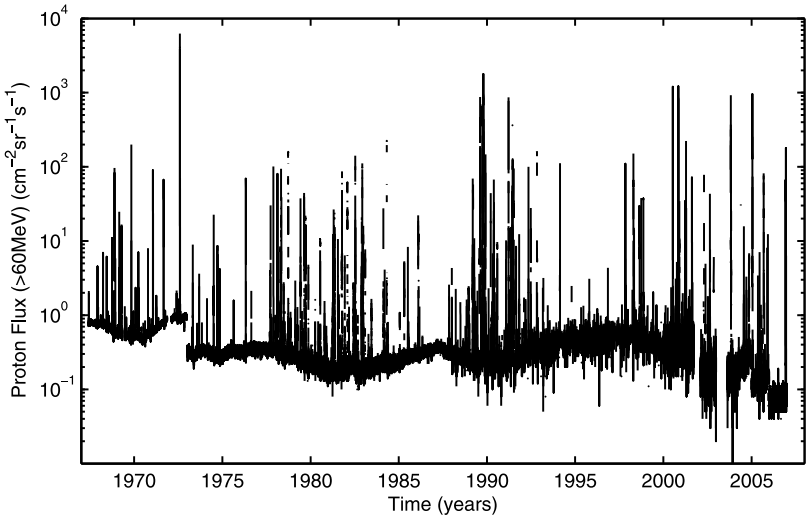

Figure 1. The hourly means of energetic proton flux (>60 MeV) as provided by the OMNI 2 data set. Data begins in May 1967, and we have employed the series up until January 2007.

employ the McMurdo Neutron monitor, because it is a homogenous and continuous record over the entire OMNI 2 proton flux record. The McMurdo NM is maintained by the Bartol Research Institute, and the data is available at http://neutronm.bartol.udel.edu/. Furthermore, this NM is at a high latitude such that the particle rigidity cutoff is set by the atmosphere, rather than the geomagnetic field, and is lower than for lower-latitude NM stations, at near 1 *GV*. Although this corresponds to an energy threshold about 16 times larger than that of the OMNI 2 60 MeV threshold, this is closer than for the lower-latitude neutron monitors. We here use 54 day medians of the proton flux ($\langle f \rangle$) to define the background because the fraction of samples within SEP events is small. The scatterplot of the 54 day medians of the OMNI 2 proton flux against the corresponding values for the McMurdo NM count rate, shown in Figure 2, reveals three distributions. These distributions have been identified with three intervals in the data set which we here term A, B and C. A is the IMP 4/5 era, B is the period from the commencement of IMP 7 to 1991, and C is from 1991 until 2001. The data for these three intervals are shown in Figure 2a by different symbols: all three give linear variations but the behavior is far from the same in all three. To test if these distributions are a feature of the proton flux or the McMurdo NM record, the analysis was repeated with the NM records from Thule, Newark and the South Pole, all also maintained by the Bartol Research Institute. For each station the proton flux revealed the three distinct distributions. A linear regression (least squares) was performed between the median proton flux and median NM count for each interval, these are displayed in Figure 2a as dashed, dot-dashed, and dotted lines for A, B and C, respectively. To homogenize the data set, each distribution was linearly transformed (i.e., adjusted in gradient and offset) so that the relationship between the distributions and the NM count was the overall mean of the regressions. The result of this is shown in Figure 2b. A linear interpolation with time was performed to fill any data gaps. The correcting coefficients G_j (gradient) and C_j (offset) are different for intervals A, B and C. In Figure 3, the periods beneath the dark, medium and light grey bars show the proton flux after these homogenizing corrections have been applied.

[13] There are two reasons why the above method cannot be applied to the OMNI 2 proton flux for the period 2001–2007. First the assumption that the background trend of the proton flux is only due to solar wind modulation of the local GCR spectrum is invalid for a geostationary satellite like GOES. Furthermore, the remaining IMP 8 data is too fragmented for the previous method to work robustly and it would still leave large data gaps to be filled. Instead, we here estimate the near-Earth heliospheric proton flux from the GOES data (made available by NOAA at http://www.ngdc.noaa.gov/stp/satellite/goes/dataaccess.html), and the McMurdo NM.

[14] This is done in two stages; the GCR background and solar proton event fluxes are estimated separately and then combined. The background is estimated by taking the McMurdo NM count and multiplying it by the mean of the regressions previously used to homogenize the IMP data. To estimate the solar proton flux in events, a relationship is established between the IMP and GOES data sets.

[15] The intended use of the final homogenized proton flux record is the determination of a database of observed gradual SEP events, with accurate calculation of event properties. Therefore it is important to consider how best to estimate the solar proton flux in these events. Due to the logarithmic nature of the variations in the proton flux during SEP events, calculations of properties such as event fluence have a stronger dependence on the event peak than on its onset and decline. To separate SEPs from background GCR protons we need to set a threshold flux. For the IMP and GOES data sets we initially tried thresholds of 2 cm^{-2} sr^{-1} s^{-1} and 0.3 cm^{-2} sr^{-1} s^{-1}, respectively. All proton flux above these thresholds was assumed to be of solar origin. Over the period 1998–2001, a linear regression was performed on the logarithms of the solar proton flux. It was discovered that the population of data points was skewed so heavily toward lower flux values that the resulting relationship did not capture the maxima of events well. This was improved upon with a modest increase in the thresholds to 20 cm^{-2} sr^{-1} s^{-1}

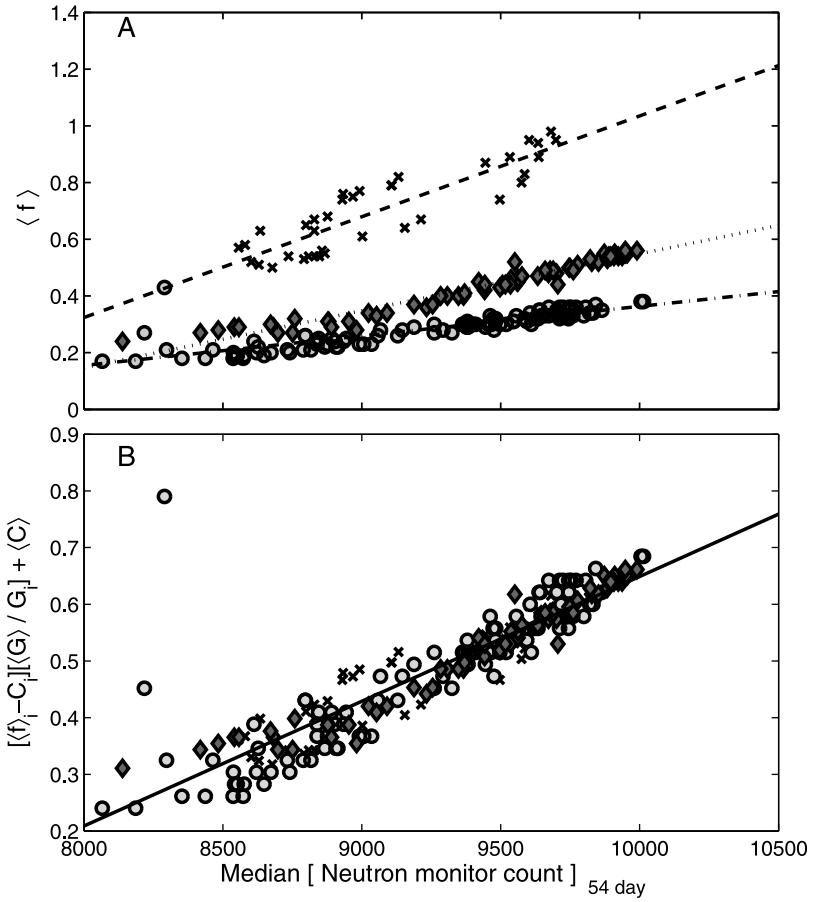

Figure 2. (a) Scatterplot of the 54 day medians of the proton flux, $\langle f \rangle$, against the 54 day medians of the neutron monitor count rate over the period 1967–2001. Crosses, circles, and diamonds denote periods A, B, and C, as described in text, and the dashed, dot-dashed, and dotted lines are the respective linear regressions for these data subsets. (b) The distribution of median flux values after homogenization (see text for details) for all three periods identified above. G_j and C_j are the gradient and offset coefficients for the three regressions on periods A, B, and C, while $\langle f_j \rangle$ is the 54 day median proton flux for those intervals. $\langle G \rangle$ and $\langle C \rangle$ are the means of the regression coefficients G_j and C_j.

and 5 cm^{-2} sr^{-1} s^{-1} (for IMP 8 and GOES 11, respectively) the resulting power law takes the form $f_i = 4.84 f_g^{0.786}$, where f_i and f_g are the simultaneous fluxes observed in interplanetary space and at geostationary orbit, respectively. Figure 4 displays a scatterplot of the data and the regressions for the different thresholds. The regression for the higher pair of thresholds (solid line) has been extrapolated to lower flux values, and in this region it is considered an adequate approximation to the regression for the lower pair of thresholds. On the other hand, the regression for the lower threshold (dashed line) is considerable in error, considering this is a log-log plot, for the large fluxes within SEP events. The higher threshold regression is therefore the more appropriate to the SEP study and is used here as it is a good approximation to the fit for lower thresholds at lower fluxes.

[16] This relationship is then used to include GOES data from the 2001 to 2007 period. All flux values above the 0.3 cm^{-2} sr^{-1} s^{-1} threshold are transformed using the power law into an estimate for the near-Earth solar proton flux. These are added to the estimate for the GCR background, and the data is interpolated to fill any resulting data gaps. The full data sequence derived this way is shown in Figure 3.

[17] In working with energetic proton flux data from both OMNI 2 and GOES it becomes apparent that there are occasionally errors in the OMNI 2 proton flux time series. At these points large proton fluxes are recorded for which no source can be identified and they are therefore considered spurious. When processing the energetic proton flux we do not attempt to suppress these errors, but note their existence. Our justification for this is that our procedure to homogenize the proton flux data is robust to their effect, and our event detection algorithm, outlined in section 2.2, explicitly excludes them from being identified as a gradual SEP event.

2.2. Event Identification

[18] Here the goal is to develop a simple algorithm to identify gradual SEP events in the homogenized data set. We employ a flux threshold and minimum duration as criteria to identify events that are large yet longer lived than impulsive events. Event onset and decline occurs at the crossing and recrossing of the flux threshold, and the event duration is the time between onset and decline. It is assumed

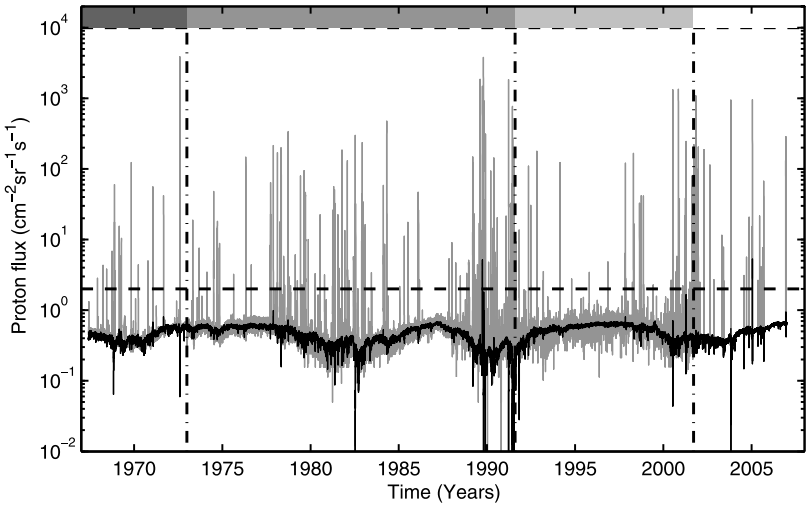

Figure 3. The data set shown in Figure 1, periods A, B, and C, respectively. The horizontal dashed line marks the 2 cm^{-2} sr^{-1} s^{-1} threshold used in the homogenization of the 2001–2006 period of proton flux and in the automated event detection. The grey line shows the homogenized proton flux, and the thick black line is the McMurdo NM count, multiplied by the mean of regressions used to homogenize the three IMP flux periods.

the homogenized proton flux record has three sources, GCRs, impulsive SEPs and gradual SEPs. If we set a suitably high threshold that excludes the GCR-associated proton fluxes, it defines "events" when this threshold is exceeded. These events may have three sources: impulsive SEPs and gradual SEPs and what may be termed false positives. The false positives have two origins. One source is the data spikes discussed in section 2.1. Additionally, variability in the proton flux can result in multiple crossings of the flux threshold during the onset and decline of a gradual or impulsive SEP event. False positives typically last for 1 h, but may persist for several hours. Impulsive and gradual SEPs have different characteristic time scales; typical time scales for gradual and impulsive events is of the order of days and hours, respectively [*Kallenrode*, 2003; *Reames*, 1999].

[19] Due to the different characteristic time scales of these three classes of event, we have investigated to see if gradual SEPs may be differentiated from impulsive SEPs and false positives by means of the event duration. The variation of the number of events as a function of duration was calculated for three flux thresholds. The duration of each event was calculated and these were counted in 3 h wide bins from 1 to 150 h. Figure 5 presents these distributions for flux thresholds of 1,2 and 3 cm^{-2} sr^{-1} s^{-1} marked by squares, circles, and triangles, respectively. We observe that, up to a duration of 50 h, the 1 cm^{-2} sr^{-1} s^{-1} threshold most often contains more events than the 2 and 3 cm^{-2} sr^{-1} s^{-1} thresholds . However, for the 2 and 3 cm^{-2} sr^{-1} s^{-1} thresholds, the number of events at each duration are in much closer agreement, particularly for durations exceeding 24 h.

[20] The event criteria should balance maximizing the number of identified gradual SEPs, while minimizing the inclusion of false positives and impulsive SEPs. The criteria chosen to identify gradual SEPs are a flux threshold of 2 cm^{-2} sr^{-1} s^{-1} and a minimum duration of 24 h. A minimum duration of 24 h will exclude all false positives, which do not persist longer than a few hours, and will also remove the large majority of impulsive SEPs. Although it is possible that a very small number of impulsive events may persist for long enough to be recorded as a gradual event, we expect this contamination to be small. A further condition adopted is that there must be greater than 50% data coverage during the event, to limit the effect that interpolation may have on

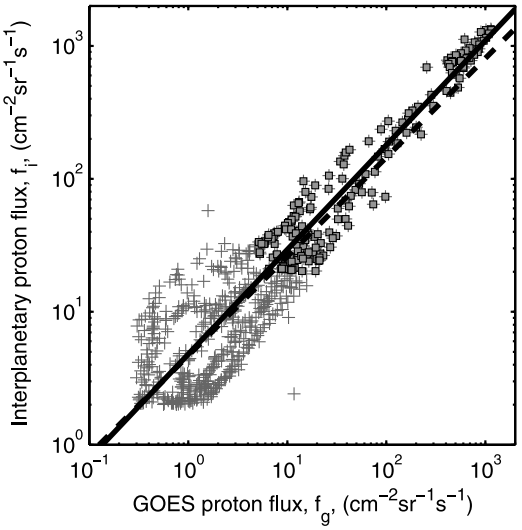

Figure 4. Comparison of the simultaneous SEP flux observations made inside and outside the Earth's magnetosphere (f_g and f_i, respectively). The grey crosses mark flux measurements above the thresholds of 2 and 0.3 cm^{-2} sr^{-1} s^{-1} for OMNI and GOES, respectively, while the squares mark the same data above thresholds of 20 and 5 cm^{-2} sr^{-1} s^{-1}. The solid black line is a linear regression on the logarithm of the fluxes above the higher pair of thresholds, and the dashed line is the same but for the lower pair of thresholds. At lower fluxes the regressions are very similar but drift apart at higher fluxes.

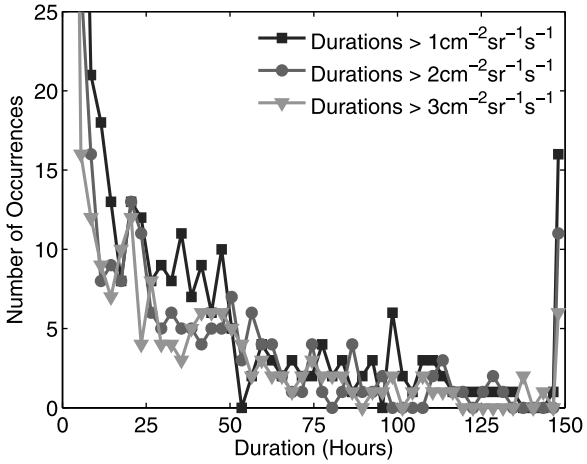

Figure 5. The variation in the number of events as a function of event duration for three flux thresholds of 1, 2, and 3 cm^{-2} sr^{-1} s^{-1}, marked by circles, squares, and triangles, respectively. The data points on the far right of the plot are for all events of duration greater than or equal to 150 h.

the calculation of event properties. Figure 6 shows two events identified using these criteria; Figure 6a is an event with complete coverage, while Figure 6b shows an event which has just over 50% coverage. Data gaps have been filled using a straight line fit to the existing data. Interpolated values are marked by crosses whereas observed fluxes identified to be in a gradual SEP event by the above criteria are shaded grey. The horizontal dashed lines give the 2 cm^{-2} sr^{-1} s^{-1} threshold. Figure 6b is a "worst case" in that the largest data gap is early in the event which means that the onset time, peak flux and fluence are poorly defined by the polynomial fit. In particular, fluence may be underestimated if there were larger fluxes during the initial data gap than the peak values observed immediately after that data gap. On the other hand, the data clearly reveal that a gradual SEP event was present and it is more useful to record an event, albeit potentially underestimated in fluence, than not. For events with <50% it becomes increasingly unclear if an event is present, or if more than one is present, or if it/they are impulsive rather than gradual in nature.

[21] However these conditions are not enough to separate out overlapping sequences of activity, where successive events are sufficiently close together in time that the flux level does not drop back down below the event threshold between them. These sequences are identified manually, and the minimum between the two events is used to separate them. Given that the minimum may be hard to define for two events that are very close together, this procedure does introduce some subjectivity and uncertainty into the estimation of the event onsets, durations and total proton fluences. After a sequence of activity is identified and separated the data coverage of each event is recalculated, and the event (s) are discarded if they fall below the 50% coverage criterion. This detection algorithm produces a database of 110 events over the era 1967–2007, which can be obtained via the supplementary material provided online.[1]

[1]Auxiliary materials are available at ftp://ftp.agu.org/apend/ja/2010JA016133.

2.3. Comparison With Other SEP Databases

[22] A number of other databases of SEP events have been produced. It is beneficial to establish the differences and similarities between the different databases, and the merit of the homogenous, gradual SEP database generated by the procedure described in sections 2.1 and 2.2. Here we will draw comparisons between some of the most frequently used SEP databases compiled from spacecraft measurements, and also a terrestrial record of SEP events.

[23] NOAA have produced a list of "Solar Proton Events Affecting the Earth Environment", which utilizes data from the GOES missions over the period January 1976 to December 2009. The algorithm used to extract events from this flux record is as follows. The 5 min average integral proton flux (>10 MeV), must be higher than 10 cm^{-2} sr^{-1} s^{-1} for 3 consecutive data points (i.e., 15 min) to trigger the start of an event. A return to less than or equal to the 10 cm^{-2} sr^{-1} s^{-1} event threshold marks the end of an event. Consequently this algorithm is well suited to detecting, but not resolving, both the short impulsive and longer-lived gradual SEP events, but may not necessarily resolve overlapping events in a sequence (note that this is not a criticism of the NOAA event detection algorithm as it was not designed for that purpose). Furthermore, the NOAA documentation is clear that, as of yet, there has been no attempt

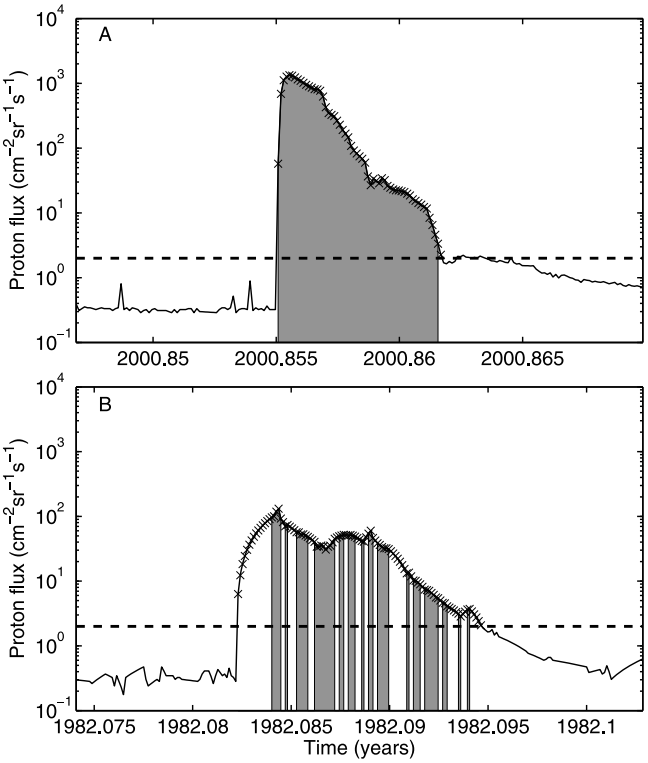

Figure 6. (a) An SEP event with complete data coverage. (b) An SEP event with just above the minimum data coverage requirement of 50%, having 56% coverage. In both cases, values exceeding the event threshold are shown by crosses. The grey shading denotes where values were observed, and crosses without shading have been interpolated using a linear interpolation.

Table 2. Comparison of the SEP Databases

	NOAA	*Rosenqvist et al.* [2005]	*Bazilevskaya et al.* [2010]	This Survey
Period of overlap with this survey	1976–2006	1974–2002	1967–2006	1967–2006
Total number of SEPs in survey during overlap	225	199	92	112
Number of coincident SEPs with this survey	82	87	84	112

to cross normalize the data sets from the variety of instruments that have contributed to the database.

[24] *Rosenqvist et al.* [2005] used the methodology that *Feynman et al.* [2002] introduced when establishing an SEP database for the JPL91 model of SEP fluence: they created an updated list of SEP events over the period January 1974 to May 2002. The data set used was a composite formed from IMP 8 and GOES integral proton flux records ($E >$ 10 MeV). Significant preprocessing is applied to the data sets, which is described in full in their paper. The event criteria are that a sequence of activity begins when the daily average proton flux rises above 1 cm^{-2} sr^{-1} s^{-1} and ends when the daily average proton flux falls below this threshold for 2 concurrent days. Furthermore, an event must have a minimum fluence of 10^7 cm^{-2}. This detection algorithm has more similarities to our method than does the NOAA algorithm. The main differences are that our method is designed to exclude impulsive SEPs, whereas the Rosenqvist et al. procedure could more readily permit impulsive SEPs to be recorded as an event. Additionally, like the NOAA methodology, the algorithm of Rosenqvist et al. does not separate out overlapping events in a sequence of activity.

[25] A database of SEP events that detectably penetrate Earth's atmosphere was recently published by *Bazilevskaya et al.* [2010]. Although supported by spacecraft measurements, most of the data were obtained from high-altitude balloon measurements of energetic proton flux at mid and polar latitudes. This record extends over the period 1957–2008. The advantage of this database is that it gives a largely independent measure of geoeffective SEPs, useful for determining the relevance of our own database for studying the terrestrial effects of SEPs. A problem with this database is that there is large, unavoidable, error associated with estimating the total fluence of an event. Enhancements in the energetic particle flux can only be reliably detected at very high altitudes, and there is a limit on the number of balloons which may be launched during a long-lived event. This restricts the data coverage of an event, making fluence estimates difficult. In addition, data on events are lost if the event starts prior to a routine flight reaching the required altitude. Nonetheless, it is an excellent record of the occurrence of events detectable in the atmosphere and spans the greatest period of time, covering the entire duration of our own database.

[26] These databases are all formed from time series at different temporal resolutions, and as such they all provide different information about the timing of events. The NOAA database provides information on the timing of the event onset and maximum activity, whereas the *Rosenqvist et al.* [2005] database states the days an event begins and ends. The *Bazilevskaya et al.* [2010] database provides the day an event begins and the times of observation. This means we cannot consistently compare all aspects of our database to the other three. To compare our database against the NOAA database, we analyzed the onset of events, associating events that occur within ±2 days. To compare our database to the Rosenqvist et al. database, we associate events when the maxima of an event in our database occurs within a start and end time of an event in Rosenqvist et al.'s list, within a ±1 day window. Finally, to compare our database against the Bazilevskaya et al. database we compared onset dates with a ±2 day window. The results are displayed in Table 2.

[27] Considering the differences in the event detection algorithms this is an encouraging result. The review of impulsive and gradual SEPs by *Kallenrode* [2003] shows that the rate of impulsive SEPs (some 10 $year^{-1}$) is comparable to the rate of gradual SEPs (≈10 $year^{-1}$). Recalling that both the NOAA and *Rosenqvist et al.* [2005] databases should be able to resolve impulsive events, which we have tried to exclude, it is reasonable that in the overlap between our databases both NOAA and Rosenqvist et al. contain roughly twice as many events as does our survey. There is a similar number of events in the overlapping period of the *Bazilevskaya et al.* [2010] database and our database. Furthermore, there is a high level of positive association between events when we compare onset dates between the databases. This agreement between our database and terrestrial observations of SEPs suggests that our database might be particularly suitable for studying the geophysical effects of SEPs.

3. Solar Cycle Variation of SEP Events for Cycles 20–23

[28] As an application of the database of gradual SEP events presented here, the distribution of SEP occurrence and fluence over the solar cycles 20–23 (C20–C23) was investigated. Displayed in Figure 7 are the SEP occurrence and fluence distributions as a function of the solar cycle phase. To determine the solar cycle phase, the Bartels rotation period mean of the sunspot number (SSN) is calculated, followed by the 15 point moving average (with equal weightings). Minima in this smoothed Bartels period mean SSN record are taken to mark the $0/2\pi$ phase points in each cycle. The phase at a time t, between the zero phase points at times t_0 and t_i, with $t_i > t_0$, is $\phi = ([t - t_0]/[t_i - t_0]) \times 2\pi$. This calculation is similar to the method presented by *Lockwood and Owens* [2003]. The solar cycle phase is divided into 12 equal width bins. For each phase bin of each solar cycle, the total number of SEPs (N_{sep}) and total fluence (F) in those N_{sep} events and mean sunspot number ($\langle SSN \rangle$) is calculated. In Figure 7, the black lines mark the total occurrence and the diamonds mark the total fluence for each phase bin, the grey histogram displays solar activity as determined by $\langle SSN \rangle$. The infrequent, stochastic nature of SEP events is apparent in each of the single solar cycle variations, with large fluctuations around the variation of SSN over the cycle. However, a composite of all observations over C20–C23 was produced, which spans almost 4

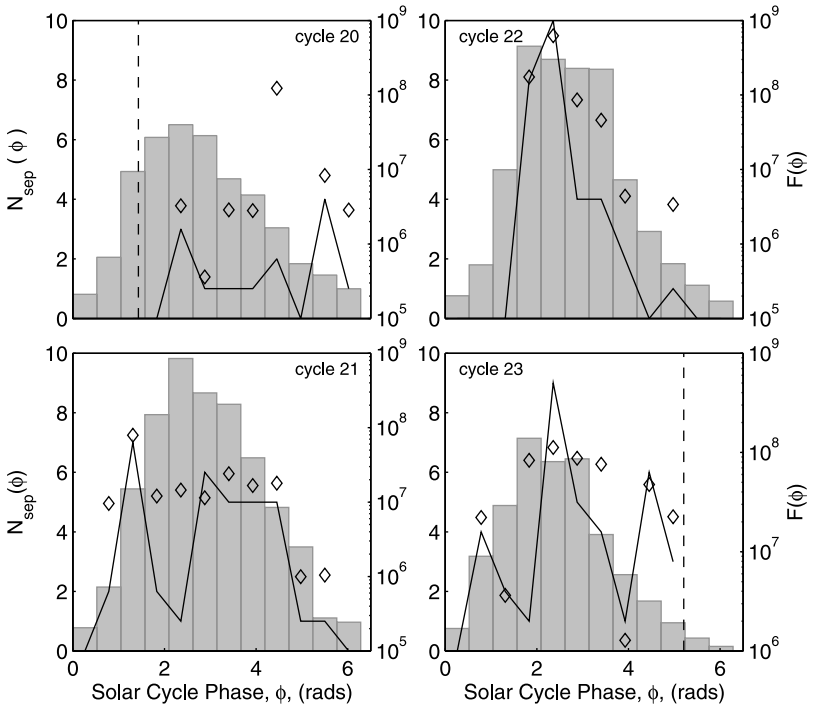

Figure 7. The variation of SEP occurrence and fluence with solar cycle phase for solar cycles 20, 21, 22, and 23. The histograms show the mean SSN for each phase bin, while the solid black line plots the SEP occurrence (N_{sep}), and diamonds mark the total SEP fluence (F). The vertical dashed lines in the first and last plots mark the beginning and end, respectively, of the energetic proton flux record.

complete solar cycles. In doing this, it is necessary to consider the phase sampling distribution. The lack of observations at the beginning of C20 and end of C23 means that the sampling of the extremes of the composite phase range is reduced. Therefore, the occurrence and fluence distributions are divided by the phase sampling distribution (i.e., the occurrence frequency (Ω_{sep}) and fluence rate (Ψ) with phase are computed), and then both are normalized. This has a relatively small effect on the distributions, as the phase sampling is essentially a constant function which tails off slowly at the extremes of phase. The result is a small suppression of the main body of the occurrence and fluence distributions and an enhancement of the tails of the distributions. Figure 8 displays this data, with the format being the same as each panel of Figure 7. Both the occurrence frequency and fluence rate show a variation more similar to that in SSN when averaged over all 4 cycles. This variation is discussed further in section 4.3.

[29] To investigate this further, the variation of SEP occurrence and fluence with both SSN and the interplanetary magnetic field magnitude (IMF) at 1 AU (B_{mag}) was calculated. For the interval of our SEP database, means over each Bartels rotation period (T_B) were determined for SSN ($\langle SSN \rangle_B$) and B_{mag} ($\langle B_{mag} \rangle_B$). It is necessary to average over solar longitudes as SEPs are guided along IMF field lines which means source regions are often at different longitudes to Earth (where they are detected). The Bartels period time scale is chosen as it is just longer than the largest time scale that might be expected for an event, but is short enough to better capture the variability in heliospheric conditions, which can start to be averaged out on longer time scales, for example annual resolution. Both $\langle SSN \rangle_B$ and $\langle B_{mag} \rangle_B$ were separated into 8 quantiles and for each quantile the SEP occurrence (N_{sep}) and logarithm of total fluence ($\log_{10}[F]$) were calculated (as it is approximately normally distributed, as discussed by *Rosenqvist et al.* [2005]). The event occurrence frequency Ω_{sep} and $\log_{10}[F]$ rate is then estimated, by dividing the N_{sep} and $\log_{10}[F]$ by the duration

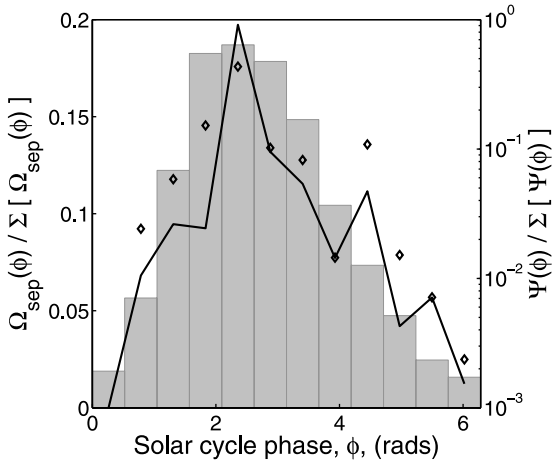

Figure 8. Variation of SEP occurrence and fluence over solar cycles 20–23. The format is the same as each panel of Figure 7; however, a complete number of cycles have not been sampled, and hence, the occurrence and fluence distributions are divided by the phase sampling distribution. $\Omega_{sep}(\phi)$ and $\Psi(\phi)$ are the occurrence frequency and fluence rate as a function of the solar cycle phase ϕ. The plotted distributions are normalized.

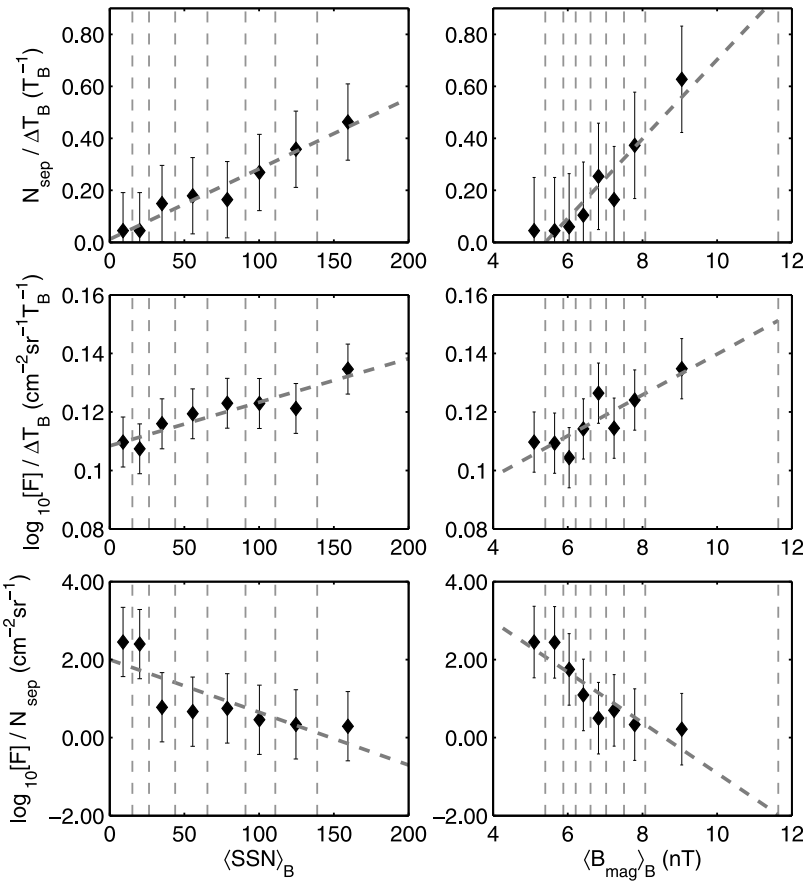

Figure 9. Plots of mean values (diamonds) with error bars of $\pm\sigma$ (where σ is the standard deviation) in eight quantiles which divide the 536 Bartels rotation periods studied equally, giving 67 in each. The vertical dashed lines mark the edges of the eight quantiles, and the thick dashed lines are linear regressions against the scattered points. (left) Mean SSN over the Bartels rotation $\langle SSN \rangle_B$ along the horizontal axis. (right) The Bartels interval means of the IMF magnitude $\langle B_{mag} \rangle_B$. The vertical axes show (top) the mean occurrence frequency per Bartels interval (T_B = 27 days in duration) where N_{sep} is the number of events in the quantile and ΔT_B is the total interval ($\Delta T_B = 67 T_B$); (middle) the log-fluence rate ($\log_{10}[F]/\Delta T_B$); and (bottom) the log-fluence per event ($\log_{10}[F]/N_{sep}$).

spanned by each quantile ΔT_B. A total of 536 Bartels periods were sampled over the SEP database, which means each of the 8 quantiles contained 67 Bartels periods, so that $\Delta T_B = 67 T_B$. Last the mean of the logarithm of the fluence in an individual event was also calculated, $\log_{10}[F] / N_{sep}$.

[30] Spearmans' rank correlation was calculated for each of the Ω_{sep}, $\log_{10}[F]$ rate and $\log_{10}[F] / N_{sep}$ versus $\langle SSN \rangle_B$ or $\langle B_{mag} \rangle_B$ combinations. The correlation coefficient (r_s) gives information on the degree to which we might expect a monotonic relationship to exist between two variables, without going so far as to assume a linear relationship. The probability that this value of r_s would be obtained when the true correlation was zero was calculated with an exact (permutation) test. Under the null hypothesis that the true value of r_s is zero, all possible orderings of the data are equally probable. The sampling distribution of r_s under the null hypothesis may therefore be established directly, by calculating r_s for every ordering of the data. Comparing the observed value of r_s, to the sampling distribution of r_s under the null hypothesis allows us to determine the probability that the observed value of r_s is a result of chance. It was found that all the calculated correlations have a <5% chance of being an artefact of statistical noise. These values are summarized in Table 3. Displayed in Figure 9 (top) are the plots of occurrence frequency against $\langle SSN \rangle_B$ and $\langle B_{mag} \rangle_B$. The solid diamonds mark the occurrence frequency ($N_{sep}/\Delta T_B$) at the mean of each quantile, while the vertical dashed lines mark the quantile edges. The error bars in the occurrence frequencies are ±1 standard deviation. The grey dashed line is a linear regression between the parameters and occurrence frequency. The coefficients of the linear regression are included in Table 3. Figure 9 (middle) shows the same analysis for the fluence rate ($\log_{10}[F]/\Delta T_B$) and Figure 9 (bottom) for the fluence per event ($\log_{10}[F]/N_{sep}$). The similarity between the behavior in the right and left columns in Figure 9 is not surprising as *SSN* and B_{mag} show solar cycle variations that have many similarities [*Hapgood et al.*, 1991]. There is a relationship, which is close to linear, between SEP occurrence frequencies and $\log_{10}[F]$ rates and solar activity, as determined from $\langle SSN \rangle_B$ and $\langle B_{mag} \rangle_B$. Furthermore, $\log_{10}[F]/N_{sep}$ decreases with increasing solar activity, which can also be fitted with a linear relationship.

Table 3. Regression Coefficients and Statistics of SEP Variation With Heliospheric Parameters[a]

$x - y$	Regression Coefficients (α, β)	r_s	p-Value
SSN − Ω_{sep}	0.0027 T_B^{-1}, 0.0116 T_B^{-1}	0.970	0.0006
SSN − $\log_{10}$[F]/ΔT_B	0.0001 $\log_{10}[F]T_B^{-1}$, 0.1084 $\log_{10}[F]T_B^{-1}$	0.881	0.0072
SSN − $\log_{10}$[F]/N_{sep}	−0.0135 $\log_{10}[F]$, 2.0004 $\log_{10}[F]$	−0.976	0.0004
Bmag − Ω_{sep}	0.1525 T_B^{-1} nT^{-1}, −0.8229 T_B^{-1}	0.970	0.0006
Bmag − $\log_{10}$[F]/ΔT_B	0.0070 $\log_{10}[F]T_B^{-1}$ nT^{-1}, 0.0699 $\log_{10}[F]T_B^{-1}$	0.833	0.0154
Bmag − $\log_{10}$[F]/N_{sep}	−0.6484 $\log_{10}[F]nT^{-1}$, 5.5701 $\log_{10}[F]$	−0.976	0.004

[a]Here x and y are the parameters correlated, the linear regression is of the form $y = \alpha x + \beta$, the correlation coefficient is r_s, and p is the probability that the correlation was found by chance.

The dependence of occurrence frequency on both *SSN* and B_{mag} is greater than the corresponding value for $\log_{10}[F]/N_{sep}$, so the net effect is that the $\log_{10}[F]$ rate increases with increasing solar activity.

4. Discussion

4.1. Implications for Current Engineering Models

[31] These results are in agreement with a study by *Nymmik* [2007], who used SEP databases produced by *Rosenqvist et al.* [2005] and *Mottl* [2005] to investigate the variation of SEP occurrence frequency with smoothed monthly mean SSN. The Rosenqvist et al. database is the one described previously, and the database produced by Mottl extracts both impulsive and gradual events and separates out sequences of overlapping activity. Nymmik performed a linear regression on the logarithm of SEP occurrence frequency and logarithm of smoothed monthly mean SSN for each database. This resulted in power laws describing the observed relationship between SEP occurrence frequency and monthly mean SSN for the Rosenqvist et al. and Mottl databases, the exponents of which were 0.95 and 0.99, respectively. Nymmik concluded that, within the limits of experimental error, a linear relationship exists between SEP occurrence frequency and solar activity.

[32] It is therefore a sensible to ask if this could have any ramifications for the improvement of SEP fluence models. Current engineering models of SEP fluence, such as the JPL-91 model produced by *Feynman et al.* [1993] and updated by *Feynman et al.* [2002] and *Rosenqvist et al.* [2005], are designed to estimate the expected fluence of SEP protons in a 1 AU orbit for different mission durations. The methodology was to develop parametric models of the occurrence and fluence of SEP events, and to use a Monte Carlo simulation to estimate the expected SEP fluence for a given mission duration and confidence level.

[33] In constructing this estimate it was established that the fluences of SEP events, integrated over a mission, for the database of SEPs available at the time, were most accurately parameterized by the lognormal distribution. Furthermore, although it was recognized in the original model that the occurrence of SEPs appears to cluster in time, to aid the calculation the occurrence of SEPs was approximated to be a Poisson process. Additionally the occurrence of SEPs was approximated to have a stationary occurrence probability for 7 years around solar maximum, and to have negligible occurrence probability for the remaining 4 years of an 11 year solar cycle.

[34] Our results from investigating the occurrence of SEPs as a function of the solar cycle phase, which are in agreement with previous work by *Nymmik* [2007], show a clear solar cycle variation of SEP occurrence. Furthermore, a study by *Jiggens and Gabriel* [2009] has also shown that there may be more accurate parameterizations of SEP occurrence than the Poisson distribution. We suggest that with the advantage of over 14 years of extra observations, it may be possible to develop a model of SEP fluence with improved parameterizations of SEP occurrence and fluence. Additionally it could be of benefit to couple this model with a measure of solar activity, which may describe variation in the parameterizations over the solar cycle phase.

4.2. The Variation of SEP Events With Heliospheric Conditions

[35] Here we aim to draw conclusions on the variation of SEP events with heliospheric conditions, placing these conclusions in the context of other works that have analyzed this phenomenon. Specifically we compare our results with studies by *McCracken et al.* [2004] and *Kahler* [2009], who separately investigated the variation of large fluence SEP events with heliospheric conditions. Here we describe these studies as relating to large fluence SEP events as both *McCracken et al.* [2004] and *Kahler* [2009] use a database of events established by *McCracken et al.* [2001] from the analysis of odd nitrogen (NO_y) deposits into polar ice, also complemented by satellite measurements. There is great variation in the quantity of nitrates in a thickness of the ice core. Impulsive depositions of nitrates precipitated down from the atmosphere (or even produced directly in the ice in a GLE) must be very large to perturb the "background" variation enough that they may be resolved. It is only SEP events from the high fluence tail of the SEP fluence distribution which may cause these detectable variations in the nitrate quantity.

[36] Using a reconstruction of the IMF magnitude at 1 AU derived from SSN, *McCracken et al.* [2004] derived an inverse relationship between an estimate for the probability of a large fluence SEP event, conditional on there being a coronal mass ejection (CME) (for solar cycles numbers −4 to 21), and the inferred IMF magnitude averaged over two solar cycles. The B_{mag} was estimated from the model of *Solanki et al.* [2000] which extrapolates the reconstruction of open solar flux by *Lockwood et al.* [1999]. This research went further, to establish that the observed relationship appeared to follow an inverse square law, and to construct a qualitative hypothesis to explain the observations. The hypothesis was that, for a constant distribution of CME propagation speeds (V_{CME}), a lower IMF magnitude corresponds to a lower Alfvén speed (V_A), which increases the flux of SEPs generated by the interplanetary shock forming

ahead of the CME, ($V_{CME} > V_A$). Furthermore, the efficiency of the particle acceleration is increased, as the enhancement of the event front Alfvén Mach number ($M_A = V_{cme}/V_A$) has a corresponding enhancement of the shock compression ratio, as described in the comprehensive review of shock acceleration by *Jones and Ellison* [1991].

[37] This hypothesis was also investigated by *Kahler* [2009], who compared both the fluence and occurrence frequency of the large fluence SEP events, with annual means of the IMF magnitude, reconstructed from cosmogenic isotopes. In this case, no relationship was found between the annual mean IMF and the fluence of an event, but a negative correlation was found between the occurrence frequency and IMF magnitude, which was stated as statistically significant.

[38] The results of our investigation do not fully support either of these findings. We have observed a positive correlation between both the occurrence frequency and fluence rate of gradual SEP events and the magnitude of the IMF at 1 AU, on a time scale of a Bartels period. However, we have also calculated that the mean fluence of individual events increases with decreasing IMF. One possible explanation suggested here is that we are observing a competition between the production rate of shock forming CMEs in the heliosphere, and the efficiency of particle acceleration upon these shocks. In this instance, it could well be the case that the probability of strong shock production and the efficiency of shock acceleration decreases with increasing solar activity, but that overall this is more than compensated for by the rate of CMEs, which increases with increasing solar activity [*Webb and Howard*, 1994; *Owens et al.*, 2011]. This picture is consistent with our results, in that we see a net increase in the occurrence and fluence of gradual SEP events with increasing solar activity, but the mean fluence per event decreases with increasing solar activity.

[39] However, differences between our results and those of *McCracken et al.* [2004] and *Kahler* [2009] may also arise due to sampling different fluence regimes of gradual SEP events. For example, in the period 1955–1998 only 7 events have met the minimum fluence threshold of 1×10^9 cm^{-2} to qualify as a large fluence SEP event in McCracken et al.'s and Kahler's studies [*Shea et al.*, 1998], of which only 2 are between 1967 and 1998 and feature in our database. Therefore the large fluence SEP events analyzed by McCracken et al. fall into the high fluence tail of the SEP event fluence distribution, and this tail may follow markedly different behaviors to the bulk of the distribution. Our studies are sampling different regimes of the SEP fluence distribution and it cannot be excluded that the discrepancies between our results are due to an evolution in the behavior of SEP events with the event magnitude. Unfortunately this is not something that can be readily tested due to the scarcity of such large SEP events in the modern era, compared to the number detected in the historic ice core data.

4.3. Evolution of SEP Events With the Solar Cycle Phase

[40] Figure 7 demonstrates that the stochastic nature of SEP occurrence (and in particular large fluence events) causes considerable variation in SEP behavior from one solar cycle to the next. However, patterns begin to come clear when all the data are averaged together, as shown in Figure 8. This plot shows that both SEP occurrence and fluence rate follow the waveform of sunspot number closely.

[41] Two main sources of gradual SEPs are expected: coronal mass ejections (CMEs) and corotating interaction regions (CIRs) (see, for example, *Gopalswamy et al.* [2002] and *Richardson* [2004], respectively). CME occurrence rate follows the sunspot cycle quite closely [*Webb and Howard*, 1994; *Owens et al.*, 2011], whereas CIRs interact with Earth much more frequently in the declining phase of the solar cycle when low-latitude extensions to polar coronal holes and isolated low-latitude coronal holes form. We note also that although CMEs may readily form shocks within 1AU [*Mann et al.*, 2003], CIRs most often do not form shocks until they have propagated out further than approximately 2 AU [*Desai et al.*, 1998]. Thus Figure 8 suggests a dominant role of CMEs in both event frequency and fluence rate. Note that although occurrence and fluence become low at solar minimum they do not consistently fall to zero, consistent with the observation that CME rates did not fall to zero, even in the recent low solar minimum [*Owens et al.*, 2011].

[42] However, close inspection of Figure 8 reveals a small second peak in the declining phase of the cycle in event occurrence and a considerable peak in the fluence rate. This implies that although CIR-driven events may be relatively rare in our database, those that are included are of relatively high fluence. In a follow-on study we will separate events that are clearly CIR related from the CME ones and compare their occurrence and properties.

5. Summary

[43] This paper has presented a method by which the homogeneity of the OMNI 2 energetic particle flux record ($E > 60$ MeV) may be improved. This was done with the aim of aiding further investigation of SEP events, in particular gradual (interplanetary shock driven) SEP events. The method employed was facilitated by use of the McMurdo neutron monitor, a long homogenous data series from which the background GCR flux may be inferred; a signal which is also present in the OMNI 2 energetic particle flux record. However, due to insufficient data coverage in the original OMNI 2 record, it was also necessary to construct an estimate for the near-Earth interplanetary energetic proton flux for the period from 2001 to 2007. To do this, the energetic particle flux is assumed to consist of two sources, GCRs from outside the heliosphere, and SEPs originating in the solar atmosphere and inner heliosphere. These two sources were estimated separately, again using the McMurdo neutron monitor but also the GOES energetic proton flux measurements provided by NOAA. The sources are then added together and joined with the homogenized OMNI 2 data. The reconstruction of events from the GOES data was done in a manner designed to ensure the event fluences were reproduced as accurately as possible.

[44] With the processed energetic proton flux record, a database of gradual SEP events was established. The emphasis of the database was to try and resolve each gradual SEP event, including overlapping events in a sequence of activity, and from this to estimate the fluence of each event. The event detection criteria differ slightly to many employed in engineering models of SEP events, where usually inte-

grated dose matters and so there is no rationale for only resolving sequences of activity into individual events, neither is there a need to make the distinction between impulsive and gradual SEPs. However, for a physical study of the SEP events, it is necessary to resolve and separate these two classes of event because the particles within them are accelerated by different physical mechanisms.

[45] The database of gradual SEP events developed in this paper was compared with the NOAA and *Rosenqvist et al.* [2005] SEP databases, used in engineering models of SEP fluence. It was also compared with a terrestrial record of SEP events, recorded by high-altitude balloon measurements of energetic particle flux. Considering the differences in the criteria used to form the different SEP databases, there was good agreement between SEP events included in our database and both the NOAA and Rosenqvist et al. database. However, there was particularly good agreement between our database and the terrestrial record of SEP events. This suggests our database may be suitable for studying the geophysical effects of gradual SEP events, for example effects on the atmosphere, on low-altitude satellites and on passengers in high-altitude aircraft.

[46] Section 4 looked at two applications of the newly developed database. The variation of SEP occurrence and fluence over the solar cycles 20 to 23 was considered, and a composite of the sampled solar cycles was formed. It was observed that SEP occurrence frequency is variable over the solar cycle. This suggests improvements can be made to SEP fluence models that approximate SEP occurrence as a Poisson process. It also suggested that there may be a relationship between solar activity as determined by SSN, and both SEP occurrence and fluence. Indeed, when this was investigated more directly by calculating the occurrence frequency and fluence rate as a function of Bartels period mean SSN, a linear relationship was found. This result is in accord with previous work by *Nymmik* [2007].

[47] Furthermore the variations of SEP occurrence frequency, fluence rate and the mean event fluence with the Bartels period means of the interplanetary magnetic field magnitude at 1 AU were calculated. We observed a positive correlation between the SEP occurrence frequency and fluence rate, and a negative correlation for the mean event fluence, as a function of the Bartels period mean IMF. These relationships were described by linear functions. It was suggested that our observations correspond to a competition between the production of strong shocks in the heliosphere, and the efficiency of particle acceleration upon these shocks. However, there are discrepancies between our results and similar studies by *McCracken et al.* [2004] and *Kahler* [2009]. Kahler found no relationship between the magnitude of large fluence SEP events and the IMF magnitude, and a negative correlation between the occurrence of large fluence SEP events and the IMF magnitude, on an annual time scale. This being the case, we note that although both studies investigate gradual SEP events, we sample different regions of the SEP fluence distribution, which may be a source of this discrepancy.

[48] Clearly gradual SEP events are a variable and important component of the near Earth space environment. The relatively scarce data afforded by the low occurrence frequency of events means that with each and every new event there can be something new to be learned about this phenomena. However, alongside developing greater understanding about SEP events themselves, it is important to further establish how these events interact with the Earth system. It is hoped that the database of gradual SEP events presented here will aid future investigations of gradual SEP events and their geophysical interactions.

[49] We have provided evidence that at lower interplanetary field strengths there are fewer gradual SEP events, but the fluence within one event is higher on average. This is significant as recent studies indicate that the data set compiled here is within a grand solar maximum that is expected to end soon [*Abreu et al.*, 2008; *Lockwood et al.*, 2009]. Indeed, *Lockwood* [2010] has estimated that there is an 8% chance of a fall to Maunder minimum conditions in the next 50 years. Extrapolation of our results into such conditions with low SSN and low B_{mag} indicates that the near-Earth space environment will become more hazardous with fewer but larger SEP events.

[50] **Acknowledgments.** We thank the many scientists who contributed to the construction of the various particle detectors and magnetometers used in this study and those who processed the data. We are particularly grateful to the Space Physics Data Facility (SPDF) of NASA's Goddard Space Flight Center for combining the data into the OMNI 2 data set, which was obtained via the GSFC/SPDF OMNIWeb interface at http://omniweb.gsfc.nasa.gov. We also thank NOAA's National Geophysical Data Centre (NGDC) for provision of the GOES data and the Bartol Research Institute of the University of Delaware for the neutron monitor data from McMurdo, Thule, Newark, and the South Pole, which is supported by NSF grant ATM-0527878. The authors also thank Matt Owens and Giles Harrison for valuable discussions of this work. The work of L.B. is supported by a studentship from the UK's Natural Environment Research Council (NERC).

[51] Philippa Browning thanks Galina Bazilevskaya and another reviewer for their assistance in evaluating this paper.

References

Abreu, J., J. Beer, F. Steinhilber, S. Tobias, and N. Weiss (2008), For how long will the current grand maximum of solar activity persist?, *Geophys. Res. Lett.*, *35*, L20109, doi:10.1029/2008GL035442.

Bazilevskaya, G. A., V. Makhmutov, Y. Stozhkov, A. Svirzhevskaya, and N. Svirzhevsky (2010), Solar proton events recorded in the stratosphere during cosmic ray balloon observations in 1957–2008, *Adv. Space Res.*, *45*, 603–613, doi:10.1016/j.asr.2009.11.009.

Desai, M. I., R. G. Marsden, T. R. Sanderson, A. Balogh, R. J. Forsyth, and J. T. Gosling (1998), Particle acceleration at corotating interaction regions in the three-dimensional heliosphere, *J. Geophys. Res.*, *103*, 2003–2014, doi:10.1029/97JA02529.

Dyer, C., F. Lei, S. Clucas, D. Smart, and M. Shea (2003), Calculations and observations of solar particle enhancements to the radiation environment at aircraft altitudes, *Adv. Space Res.*, *32*, 81–93, doi:10.1016/S0273-1177(03)90374-7.

Dyer, C., et al. (2009), Advances in measuring and modeling the atmospheric radiation environment, *IEEE Trans. Nucl. Sci.*, *56*, 3415–3422, doi:10.1109/TNS.2009.2032185.

Feynman, J., G. Spitale, J. Wang, and S. Gabriel (1993), Interplanetary proton fluence model: JPL 1991, *J. Geophys. Res.*, *98*, 281–294, doi:10.1029/92JA02670.

Feynman, J., A. Ruzmaikin, and V. Berdichevsky (2002), The JPL proton fluence model: An update, *J. Atmos. Sol. Terr. Phys.*, *64*, 1679–1686, doi:10.1016/S1364-6826(02)00118-9.

Finch, I., and M. Lockwood (2007), Solar wind–magnetosphere coupling functions on timescales of 1 day to 1 year, *Ann. Geophys.*, *25*, 495–506.

Forbush, S. (1946), Three unusual cosmic-ray increases possibly due to charged particles from the Sun, *Phys. Rev.*, *70*, 771–772, doi:10.1103/PhysRev.70.771.

Gopalswamy, N., S. Yashiro, G. Michałek, M. Kaiser, R. Howard, D. Reames, R. Leske, and T. von Rosenvinge (2002), Interacting coronal mass ejections and solar energetic particles, *Astrophys. J.*, *575*, L103–L107, doi:10.1086/341601.

Gubby, R., and J. Evans (2002), Space environment effects and satellite design, *J. Atmos. Sol. Terr. Phys.*, *64*, 1723–1733, doi:10.1016/S1364-6826(02)00122-0.

Hapgood, M., M. Lockwood, G. Bowe, D. Willis, and Y. Tulunay (1991), Variability of the interplanetary medium at 1 AU over 24 years: 1963–1986, *Planet. Space Sci.*, *39*(3), 411–423, doi:10.1016/0032-0633(91)90003-S.

Jackman, C., D. Marsh, F. Vitt, R. Garcia, C. Randall, E. Fleming, and S. Frith (2009), Long-term middle atmospheric influence of very large solar proton events, *J. Geophys. Res.*, *114*, D11304, doi:10.1029/2008JD011415.

Jiggens, P., and S. Gabriel (2009), Time distributions of solar energetic particle events: Are SEPEs really random?, *J. Geophys. Res.*, *114*, A10105, doi:10.1029/2009JA014291.

Jones, F., and D. Ellison (1991), The plasma physics of shock acceleration, *J. Geophys. Res.*, *58*, 259–346, doi:10.1007/BF01206003.

Kahler, S. (2009), Variation of SEP event occurence with heliospheric magnetic field magnitudes, *Adv. Space Res.*, *43*, 1423–1428, doi:10.1016/j.asr.2009.01.039.

Kallenrode, M.-B. (2003), Current views on impulsive and gradual solar energetic particle events, *J. Phys. G*, *29*, 965–981, doi:10.1088/0954-3899/29/5/316.

Lockwood, M. (2010), Solar change and climate: An update in the light of the current exceptional solar minimum, *Proc. R. Soc. A*, *466*, 303–329, doi:10.1098/rspa.2009.0519.

Lockwood, M., and M. Owens (2003), The accuracy of using the Ulysses result of the spatial invariance of the radial heliospheric field to compute the open solar flux, *Astrophys. J.*, *701*, 964–973, doi:10.1088/0004-637X/701/2/964.

Lockwood, M., R. Stamper, and M. Wild (1999), A doubling of the Sun's coronal magnetic field during the past 100 years, *Nature*, *399*, 437–439, doi:10.1038/20867.

Lockwood, M., A. Rouillard, and I. Finch (2009), The rise and fall of open solar flux during the current grand solar maximum, *Astrophys. J.*, *700*, 937–944, doi:10.1088/0004-637X/700/2/937.

Mann, G., A. Klassen, H. Aurass, and H.-T. Classen (2003), Formation and development of shock waves in the solar corona and the near-Sun interplanetary space, *Astron. Astrophys.*, *400*, 329–336, doi:10.1051/0004-6361:20021593.

McCracken, K., G. Dreschhoff, E. J. Zeller, D. Smart, and M. Shea (2001), Solar cosmic ray events for the period 1561–1994: 1. Identification in polar ice, 1561–1950, *J. Geophys. Res.*, *106*, 21,585–21,598, doi:10.1007/s11207-005-5257-2.

McCracken, K., G. Dreschhoff, D. Smart, and M. Shea (2004), A study of the frequency of occurence of large-fluence solar proton events and the strength of the interplanetary magnetic field, *Sol. Phys.*, *224*, 359–372, doi:10.1007/s11207-005-5257-2.

Mertens, C., B. Kress, M. Wiltberger, S. R. Blattnig, T. S. Slaba, S. Solomon, and M. Engel (2010), Geomagnetic influence on aircraft radiation exposure during a solar energetic particle event in October 2003, *Space Weather*, *8*, S03006, doi:10.1029/2009SW000487.

Mlynczak, M., et al. (2003), The natural thermostat of nitric oxide emission at 5.3 μm in the thermosphere observed during the solar storms of April 2002, *Geophys. Res. Lett.*, *30*(21), 2100, doi:10.1029/2003GL017693.

Mottl, D. (2005), The energy spectra of protons in solar energetic particle events and the problems of the experimental data reliability, Ph.D. thesis, Phys.-Math. Sci., Moscow State Univ., Moscow.

Nymmik, R. (2007), To the problem on the regularities of solar energetic particle events occurrence, *Adv. Space Res.*, *40*, 321–325, doi:10.1016/j.asr.2007.02.013.

Owens, M. J., N. U. Crooker, and M. Lockwood (2011), How is open solar magnetic flux lost over the solar cycle?, *J. Geophys. Res.*, *116*, A04111, doi:10.1029/2010JA016039.

Reames, D. (1998), Solar energetic particles: Sampling coronal abundances, *Space Sci. Rev.*, *85*, 327–340.

Reames, D. (1999), Particle acceleration at the Sun and in the heliosphere, *Space Sci. Rev.*, *90*, 413–491, doi:10.1023/A:1005105831781.

Reames, D. (2002), Magnetic topology of impulsive and gradual solar energetic particle events, *Astrophys. J.*, *571*, 63–66.

Richardson, I. (2004), Energetic particles and corotating interaction regions in the solar wind, *Space Sci. Rev.*, *111*, 267–376, doi:10.1023/B:SPAC.0000032689.52830.3e.

Rosenqvist, L., D. Boscher, S. Bourdarie, E. Daly, H. Evans, M. Hapgood, A. Hilgers, R. Stamper, and R. Zwickl (2005), Toolkit for updating interplanetary proton cumulated fluence models, *J. Spacecr. Rockets*, *42*, 1077–1090, doi:10.2514/1.8211.

Seppälä, A., C. Randall, M. Clilverd, E. Rozanov, and C. Rodger (2009), Geomagnetic activity and polar surface air temperature variability, *J. Geophys. Res.*, *14*, A10312, doi:10.1029/2008JA014029.

Shea, M., and D. Smart (2004), The use of geophysical data in studies of the historical solar-terrestrial environment, *Sol. Phys.*, *224*, 483–493, doi:10.1007/s11207-005-4138-z.

Shea, M., D. Smart, and G. Dreschhoff (1998), Identification of major proton fluence events from nitrates in polar ice cores, *Radiat. Meas.*, *30*, 309–316, doi:10.1016/S1350-4487(99)00057-8.

Solanki, S., M. Schüssler, and M. Fligge (2000), Evolution of the Sun's large-scale magnetic field since the Maunder minimum, *Nature*, *408*, 445–447, doi:10.1038/35044027.

Townsend, L., J. Shinn, and J. Wilson (1991), Interplanetary crew exposure estimates for the August 1972 and October 1989 solar particle events, *Radiat. Res.*, *126*, 108–110.

Webb, D., and R. Howard (1994), The solar cycle variation of coronal mass ejections and the solar wind mass flux, *J. Geophys. Res.*, *99*, 4201–4220.

Zharkova, V., and M. Gordovskyy (2004), Particle acceleration asymmetry in a reconnecting nonneutral current sheet, *Astrophys. J.*, *604*, 884–891.

L. Barnard and M. Lockwood, Department of Meteorology, University of Reading, Reading RG6 6BB, UK. (luke.barnard@student.reading.ac.uk)